Engineering and Technology Journal e-ISSN: 2456-3358

Volume 10 Issue 11 November-2025, Page No.- 7729-7741

DOI: 10.47191/etj/v10i11.05, I.F. – 8.482

Assessment of Surface Water and Groundwater Quality Impacts at Iduapriem Mine, Tarkwa, Southwestern Ghana Approaches for Decommissioning of a Tailings Storage Facility

Daniel Oppong

University of Mines and Technology Tarkwa Ghana

ABSTRACT: This study evaluated the hydrochemistry, surface water and groundwater quality, potential impacts, and decommissioning strategies for the Tailings Storage Facility (GTSF) at Iduapriem Mine in Tarkwa, Ghana, focusing on compliance with Ghana's Minerals and Mining Regulations (L.I. 2182). The research spanned from 2011 (baseline pre-operational year) through 2023 and aimed to assess water quality evolution, identify hydrochemical processes, and develop effective TSF closure strategies. Hydrochemical analysis was conducted on 46 sampling points comprising decant water (1), topliner sumps (19), underliner sumps (10), deep boreholes (7), shallow boreholes (7), and surface water sites (2). Results showed that multiple physical (pH, TSS, turbidity), chemical (potassium, free cyanide, nitrite, nitrate, ammonia), and trace metal (arsenic, lead, iron, copper, manganese, magnesium) parameters exceeded Environmental Protection Agency (EPA), Ghana Standards Authority (GSA), and World Health Organization (WHO) permissible limits in both surface and groundwater systems. Groundwater and surface water chemistry were predominantly characterized by Ca-HCO_3 facies, driven by carbonate and silicate mineral weathering processes. Nine distinct hydrochemical facies were identified, with Ca-HCO_3 (26%) being the most prevalent, followed by Mg-SO_4 (23%) and Ca-SO_4 (13%). Gibbs diagrams confirmed rock-water interaction as the primary controlling mechanism for water chemistry. Principal Component Analysis (PCA) identified pH, electrical conductivity, total dissolved solids, nitrate, nitrite, ammonia, iron, manganese, sulphate, and cyanide as dominant parameters contributing to hydrochemical variability. Bivariate plots revealed strong positive correlations ($r = 0.996–0.999$) between major ions, confirming the concurrent influence of silicate weathering and carbonate dissolution. Hydrochemical facies correlation analysis revealed significant geochemical interactions among topliners, underliners, shallow and deep boreholes, and surface water, indicating hydraulic connectivity and seepage migration pathways between the TSF and surrounding aquifers. Based on these findings, six integrated decommissioning approaches are recommended: systematic dewatering and water management, advanced multi-stage water treatment, recycling and controlled discharge, encapsulation with 500 mm topsoil cover, establishment of vegetated buffer zones around surface water bodies, and implementation of long-term monitoring and maintenance programs to ensure environmental protection and regulatory compliance.

KEYWORDS: hydrochemistry, mineral dissolution, water-rock interaction,ion exchange, decommissioning strategies

1. Introduction

Mining is a significant contributor to Ghana's economy, providing jobs and revenue through taxes, royalties, and exports of minerals such as gold and diamonds. However, the environmental impact of mining particularly the management of Tailings Storage Facilities (TSFs) poses major challenges. TSFs, which store waste from mineral processing, can lead to groundwater and surface water contamination due to seepage. Groundwater contamination is of grave concern where it feeds surface streams or lakes. Excessive seepage from TSFs can therefore lead to serious environmental problems such as surface and groundwater pollution (Franks et al., 2011).

To mitigate these issues, Ghana's Minerals and Mining Regulations (L.I. 2182) require measures to prevent water infiltration, ensure long-term stability of TSFs, and manage effluent within approved limits. Accordingly, this research aims to: (1) assess surface and groundwater quality; (2) determine hydrochemical facies; (3) identify factors controlling water chemistry; (4) evaluate TSF impacts on water resources; and (5) develop effective decommissioning strategies for TSFs.

2. STUDY AREA OVERVIEW

Iduapriem Mine, situated approximately 10 km south of Tarkwa and about 320 km west of Accra (Figure 1), lies within the wet semi-equatorial climatic zone. The area is characterized by a prolonged rainy season extending from March to November, followed by a brief dry season from December to February. The mean annual rainfall is approximately 1,500 mm (Al-Hassan, 2007). Temperatures typically range between 26 °C and 30 °C during the wet season and between 31 °C and 33 °C in the dry season, accompanied by consistently high humidity throughout the year. The terrain is gently undulating, with elevations

reaching up to about 300 m above sea level.

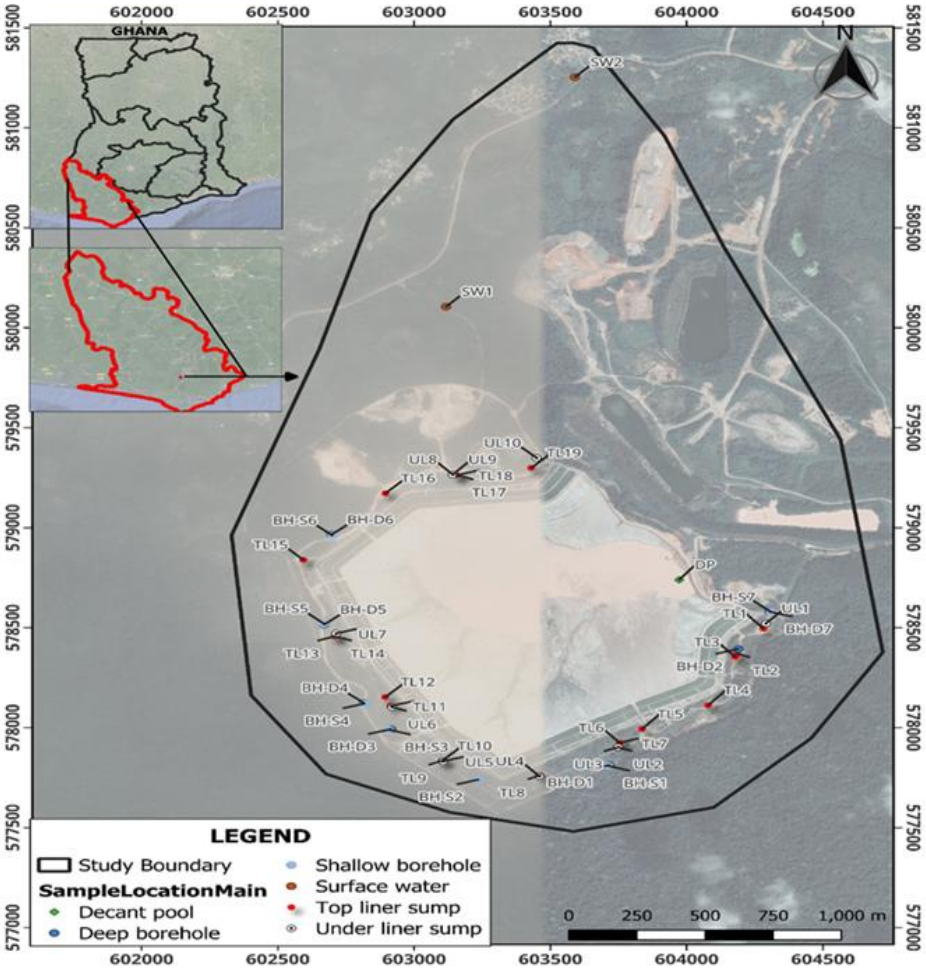

Fig.1. Location Map of Iduapriem Mine

3. MATERIALS AND METHODS

3.1 Sample collection and analysis

This study utilized a comprehensive dataset comprising both primary and secondary data obtained from multiple sources associated with the Tailings Storage Facility (TSF) of Iduapriem Mine. A total of 46 sampling locations were investigated, consisting of seven deep boreholes (70 m depth), seven shallow boreholes (30 m depth), nineteen topliner sumps, ten underliner sumps, two surface water sites, and one decant water pool. The temporal scope of the dataset spanned from 2011 established as the baseline pre-operational year through to 2023.

Primary data collection employed calibrated Horiba Multi-parameter (U-52) probes, following standardized quality assurance procedures. To minimize cross-contamination, disposable gloves were used for each sample. Prior to sampling, boreholes were pumped for approximately ten minutes to purge stagnant water and obtain representative aquifer samples (Sunkari et al., 2020). Groundwater samples were collected using bailers in accordance with purging protocols to ensure that in-situ conditions were accurately represented.

Sample preservation was undertaken immediately after collection: pH was adjusted to below 2 using 1% HNO_3 for metal analysis, samples for cyanide determination were stabilized with NaOH to maintain pH values above 12, and all samples were filtered through 0.45 µm membrane filters. Each sample bottle was clearly labelled with details including the location, date, and target analytes. Samples were transported under controlled conditions to the AngloGold Ashanti Iduapriem Environmental Laboratory, Tarkwa, Ghana, for hydrochemical analysis.

Major cations and anions; potassium (K^+), sodium (Na^+), calcium (Ca^{2+}), magnesium (Mg^{2+}), chloride (Cl^-), bicarbonate (HCO_3^-), nitrate (NO_3^-), and sulphate (SO_4^{2-}) were quantified using a HACH DR6000 spectrophotometer. Concentrations of heavy metals such as Fe, Mn, Pb, Cu, Cd, Hg, As, Zn, and Mg were determined using Inductively Coupled Plasma Optical Emission Spectrometry (ICP–OES). Principal Component Analysis (PCA) was applied to reduce the dimensionality of the large geochemical dataset and identify relationships among the chemical parameters. The Kaiser Criterion (eigenvalue ≥ 1) was adopted to determine the number of significant factors, and varimax rotation was applied to maximize variance and enhance interpretability.

Saturation indices were computed to evaluate the influence of interpretations were carried out using AquaChem software (Version 4.0), where Piper trilinear diagrams were employed to classify hydrochemical facies and Gibbs plots were used to identify dominant processes controlling groundwater chemistry (Gibbs, 1970).

As geochemical data are typically non-normally distributed, the dataset underwent a centered log-ratio (CLR) transformation following the approach of Aitchison and Greenacre (2002) to achieve normality and improve statistical reliability. Further data analysis involved multivariate statistical techniques, including factor analysis using SPSS, mineral weathering on groundwater chemistry. Geochemical to delineate key geochemical processes and contaminant interactions (Li et al., 2015; Zango et al., 2019).

Based on hydrochemical and statistical assessments, seven key decommissioning strategies were proposed to mitigate environmental risks: dewatering, treatment, recycling, encapsulation, establishment of buffer zones, long-term care, and continuous monitoring. These comprehensive analyses facilitated the interpretation of geochemical evolution and provided insights into the overall impact of tailings on both surface and groundwater systems within the TSF area (Sunkari et al., 2023

4 Results and Discussion

4.1 Quality of TSF Water, Surface Water and Groundwater

The results of the physical and chemical characteristics of decant water, surface and groundwater are presented in Tables 1 and 2. The water quality parameters show laboratory results for 2011 and 2023, representing commencement of operation of the TSF and current status respectively. The results of the various parameters were compared with the Ghana Standards Authority (GSA), EPA and WHO permissible limits. Those exceeding regulatory standards have been highlighted in Tables 1 and 2, yellow represents values exceeding WHO standards, red indicates exceedances of both WHO and EPA/GSA standards, and blue highlights parameters exceeding EPA/GSA standards.

Table 1 presents water quality results from physical, chemical, and trace metal parameters of groundwater (deep and shallow) and surface water (SW1 and SW2) in 2011. Key exceedances include pH (5.82) in shallow boreholes, with a 6% exceedance, potassium at 7 mg/L and 13 mg/L in SW2 and shallow boreholes (5% exceedance), and nitrite in SW1 at 9.580 mg/L (15% exceedance). Other exceedances include ammonia (2.75 mg/L), magnesium in SW1 (2.96 mg/L, 48% exceedance), iron in SW1 (1.13 mg/L, 36% exceedance), and SW2 exceeding limits for arsenic, magnesium, iron, and manganese with exceedances ranging from 5% to 28%. Shallow groundwater showed exceedances for lead, magnesium, iron, manganese, and copper, with exceedance percentages ranging from 2% to 28%. The physical parameters for surface water where within the range of WHO and EPA/GSA standards. Chemical data were also within the range of the standards excepts for NO_3 (3.147mg/l) and NH_3. (2.75mg/l), with a personage exceedance of 15% and 6% respectively. Trace metals however showed the most deviation from the standards. Magnesium was found to have high values in both surface (SW1 and SW2) and groundwater (Deep and Shallow) than GSA/EPA standards but with a 0% percentage exceedance. Iron with 36% percentage had values higher than the WHO standards in surface (SW1 and SW2) and much higher in the groundwater (deep and shallow) with values ranging from 5.09mg/l to 8.42mg/l. Manganese was greater than the GSA/EPA standards in SW1 (surface water) and groundwater (deep and shallow) with a 0% percentage exceedance.

Table 2 presents the water quality data for 2023. Surface water results showed exceedances mainly in turbidity and trace metals. SW2 recorded a turbidity exceedance of 99 NTU (92%). For trace metals, magnesium was elevated in both SW1 (5.1 mg/L, 91%) and SW2 (7.8 mg/L, 93%). Iron exceeded limits at 2 mg/L in SW1 (94%) and 0.6 mg/L in SW2 (89%). Manganese (92%) and copper (91%) also exceeded standards in SW2.

Groundwater recorded pH values below EPA/GSA and WHO standards, with exceedances of 92% for deep groundwater (pH 5.44) and 92% for shallow groundwater (pH 5.82). Shallow groundwater also exceeded limits for potassium (12.6 mg/L, 95%), free cyanide (93%), nitrite (94%), nitrate (92%), and ammonia (90%). For trace metals, deep groundwater recorded high levels of magnesium (19.4 mg/L, 96%), iron (11.8 mg/L, 95%), and manganese (0.26 mg/L, 90%). Shallow groundwater exceeded limits for magnesium (94%), iron (93%), copper (92%), arsenic (91%), and lead (90%).

For TSF water, the decant pool recorded the most significant exceedances, with pH (10.07, 95%), total suspended solids (1770 mg/L, 96%), and turbidity (5288 NTU, 96%). Chemical exceedances included potassium (13 mg/L in the Underliner, 96%), free cyanide (93%), nitrite (94%), nitrate (92%), and ammonia (90%). For trace metals, the decant pool showed exceedances for copper (92%), arsenic (90%), lead (89%), and cadmium (88%). The Topliner recorded exceedances for pH (91%), electrical conductivity (89%), total suspended solids (95%), turbidity (94%), and trace metals including iron (94%), manganese (92%), copper (91%), arsenic (90%), and lead (89%).

Table 1. Results of 2011 Surface Water and Groundwater Quality Parameters

2011

Physical Parameters

Parameters	GSA/EPA standards	WHO standards	Percentage of Exceedance(%)	Surface water SW 1 Min	SW 1 Max	SW 1 Average	SW 2 Min	SW 2 Max	SW 2 Average	Groundwater Deep Min	Deep Max	Deep average	Shallow Min	Shallow Max	Shallow Average
p H	6-9	6.5-8.5	6	7.16	7.61	7.34	6.86	7.42	7.24	6.60	7.88	7.06	5.82	7.93	6.91
EC (µS/cm)	1500	2500	0	164	229	207	230	464	344	49	330	175	38	696	267
TDS (mg/L)	1000	1000	0	310	463	412	105	284	176	24	188	88	18	373	142
TSS (mg/l)	50		0	9	17	13	6	24	33	3	12	6	1	13	5.3
TURB. (NTU)	75		0	19	63	48	12	54	22	2	21	10	7	18	11

Chemical Parameters

Parameters	GSA/EPA standards	WHO standards	Percentage of Exceedance(%)	Surface water SW 1 Min	SW 1 Max	SW 1 average	SW 2 Min	SW 2 Max	SW 2 Average	Groundwater Deep Min	Deep Max	Deep Average	Shallow Min	Shallow Max	Shallow Average
Sodium (mg/L)		200	0	58	68	63	4	4	4	4	18	10	11	24	11
Potassium (mg/L)	5	12	5	5	5	5	2	7	5	1	4	2	4	13	4
Calcium (mg/L)	250	200	0	5	13	9	5	5	5	8	51	26	18	50	18
Bicarbonate (mg/L)			0	32	46	39	5	13	9	8	56	26	30	100	30
Chloride (mg/L)	250	1000	0	19	20	19	38	46	42	4	14	8	17	56	17
Sulphate (mg/L)	300	400	0	29	35	32	16	19	29	1	27	7	6	16	6
CN-Fr (mg/L)	0.2		0	0.0001	0.0001	0.0001	0.0020	0.0120	0.0045	0.0041	0.0039	0.0008	0.0020	0.0080	0.0048
N-NO2 (mg/L)		3	15	0.010	9.580	3.147	0.007	2.687	2.112	0.001	0.007	0.005	0.002	0.212	0.012
N-NO3 (mg/L)	50		0	1.460	5.410	3.522	0.120	19.150	13.904	0.004	0.144	0.085	0.013	0.408	0.149
N-NH3 (mg/L)	1		6	0.04	2.75	0.66	0.02	0.28	0.07	0.01	0.06	0.45	0.07	0.20	0.17

Metals

Parameters	GSA/EPA standards	WHO standards	Percentage of Exceedance(%)	Surface water SW 1 Min	SW 1 Max	SW 1 Average	SW 2 Min	SW 2 Max	SW 2 Average	Groundwater Deep Min	Deep Max	Deep Average	Shallow Min	Shallow Max	Shallow Average
Arsenic (mg/L)	0.1	0.01	5	0.0034	0.0067	0.0049	0.0012	0.0115	0.0036	0.0007	0.0021	0.0013	0.0010	0.0026	0.0018
lead (mg/L)	0.1	0.01	7	0.0013	0.0044	0.0030	0.0024	0.0054	0.0033	0.0009	0.0025	0.0015	0.0019	0.020	0.0101
Magnesium (mg/L)	2	100	0	1.92	2.96	2.24	5.76	7.82	6.67	0.31	2.42	0.90	0.28	10.75	2.35
Iron (mg/L)	10	0.3	36	0.09	1.12	0.41	0.11	0.63	0.32	5.09	8.42	6.76	3.00	7.10	5.05
Manganese (mg/L)	0.2		0	0.010	0.110	0.081	0.013	2.761	1.387	1.120	3.967	2.540	0.079	0.689	0.261
Copper (mg/L)	5	0.05	2	0.004	0.009	0.01	0.003	0.010	0.005	0.035	0.004	0.042	0.006	0.11	0.046
Cadmium (mg/L)	0.1	0.003	0	0.000575	0.027273	0.005	0.001	0.010	0.004	0.001	0.004	0.003	0.001	0.003	0.001
Zinc (mg/L)	10	5	0	0.043033	0.551	0.34	0.0004	0.14	0.11	0.001	0.002	0.001	0.004	0.092	0.053
Mercury (mg/L)	0.005	0.006	0	0.0004	0.0034	0.0015	0.0003	0.0004	0.0003	0.001	0.004	0.0014	0.0006	0.0031	0.0010

Table 2. Results of 2023 Water Quality Parameters

2023

Physical Parameters

Parameters	GSA/EPA Standards	WHO Standards	Percentage of Exceedance(%)	Surface Water SW 1 Min	SW 1 Max	SW 1 Average	SW 2 Min	SW 2 Max	SW 2 Average	Groundwater Deep Min	Deep Max	Deep Average	Shallow Min	Shallow Max	Shallow Average
p H	6-9	6.5-8.5	92	6.68	6.84	6.77	6.87	7.15	7.02	5.44	7.05	6.48	5.82	7.93	6.86
EC (µS/cm)	1500	2500	12	399	457	428	462	673	609	141	555	337	38	696	376
TDS (mg/L)	1000	1000	0	179	216	197	297	432	384	91	347	213	18	373	224
TSS (mg/l)	50		93	8	17	12.5	1	99	23	3	12	6	9	12	10.5
TURBIDITY(NTU)	75		95	14	23	18	4	234	41	2.4	21	10	14	2	8

Chemical Parameters

Parameters	GSA/EPA Standards	WHO Standards	Percentage of Exceedance(%)	Surface Water SW 1 Min	SW 1 Max	SW 1 Average	SW 2 Min	SW 2 Max	SW 2 Average	Groundwater Deep Min	Deep Max	Deep Average	Shallow Min	Shallow Max	Shallow Average
Sodium (mg/L)		200	0	58	68	63	4	4	4	4	18	10	11	24	11
Potassium (mg/L)	5	12	5	2	9	5	3	10	7	1	4	2	4	13	4
Calcium (mg/L)	250	200	0	5	13	9	5	5	5	8	51	26	18	50	18
Bicarbonate (mg/L)			0	32	46	39	5	13	9	8	56	26	30	100	30
Chloride (mg/L)	250	1000	0	19	20	19	38	46	42	4	14	8	17	56	17
Sulphate (mg/L)	300	400	0	29	35	32	16	19	29	1	27	7	6	16	6
CN-Fr (mg/L)	0.2		96	0.002	0.002	0.002	0.000	0.001	0.001	0.001	0.005	0.003	0.001	0.027	0.008
N-NO2 (mg/L)		3	58	0.018	16.090	6.654	0.307	27.687	4.112	0.001	0.108	0.014	0.082	7.120	0.205
N-NO3 (mg/L)	50		59	1.540	7.400	4.470	0.120	19.150	13.904	0.004	1.092	0.193	0.013	0.408	0.129
N-NH3 (mg/L)	1		46.0	0.03	0.07	2.5	0.9	1.0	0.1	0.0	0.8	0.7	0.01	1.2	0.9

Metals Parameters

Parameters	GSA/EPA Standards	WHO Standards	Percentage of Exceedance(%)	Surface Water SW 1 Min	SW 1 Max	SW 1 Average	SW 2 Min	SW 2 Max	SW 2 Average	Groundwater Deep Min	Deep Max	Deep Average	Shallow Min	Shallow Max	Shallow Average
Arsenic (mg/L)	0.1	0.01	10	0.001	0.004	0.003	0.001	0.010	0.004	0.0004	0.004	0.002	0.001	0.046	0.002
lead (mg/L)	0.1	0.01	12	0.0003	0.0004	0.0003	0.0024	0.0054	0.0033	0.0008	0.0302	0.0078	0.0007	0.0910	0.0019
Magnesium (mg/L)	2	100	61	3.2	5.1	4.2	5.8	7.8	6.7	0.3	19.4	9.0	0.3	10.7	4.5
Iron (mg/L)	10	0.3	59	0.2	2.0	0.7	0.1	0.6	0.3	7.2	11.8	10.6	0.2	0.7	0.3
Manganese (mg/L)	0.2		0	0.0020	0.0032	0.0026	0.0040	0.9900	0.0825	0.0030	0.2600	0.1070	0.0009	0.0045	0.0016
Copper (mg/L)	5	0.05	8	0.007	0.010	0.009	0.001	0.5	0.022	0.001	0.004	0.001	0.001	0.1	0.040
Cadmium (mg/L)	0.1	0.003	0	0.001	0.005	0.002	0.001	0.010	0.004	0.001	0.004	0.003	0.001	0.027	0.008
Zinc (mg/L)	10	5	0	0.07	0.12	0.09	0.0004	5.14	0.91	0.9	1.0	0.1	0.009	0.07	0.029875
Mercury (mg/L)	0.005	0.006	0	0.001	0.003	0.002	0.0003	0.0005	0.0003	0.001	0.004	0.0024	0.0004	0.003	0.002

4.2 Schoeller diagrams

Schoeller diagrams (Fig. 2) were employed to illustrate the distribution patterns of major ions in decant water, surface water, and groundwater for the years 2011, 2016, 2017, and 2023. The 2011 Schoeller diagram (Fig. 2) depicts the major ion composition of groundwater (both deep and shallow) and surface water (SW1 and SW2). The highest cation concentration was recorded for calcium (Ca^{2+}) at 45 mg/L, while bicarbonate (HCO_3^-) exhibited the highest anion

concentration at 55 mg/L.

By 2023, calcium (Ca^{2+}) remained the dominant cation, with a maximum concentration of 118 mg/L, and bicarbonate (HCO_3^-) continued to be the prevailing anion, with a peak concentration of 60 mg/L. The Schoeller plots consistently indicate that Ca^{2+} and HCO_3^- are the predominant cation and anion, respectively, suggesting a hydrochemical regime primarily influenced by carbonate weathering and limited anthropogenic alteration.

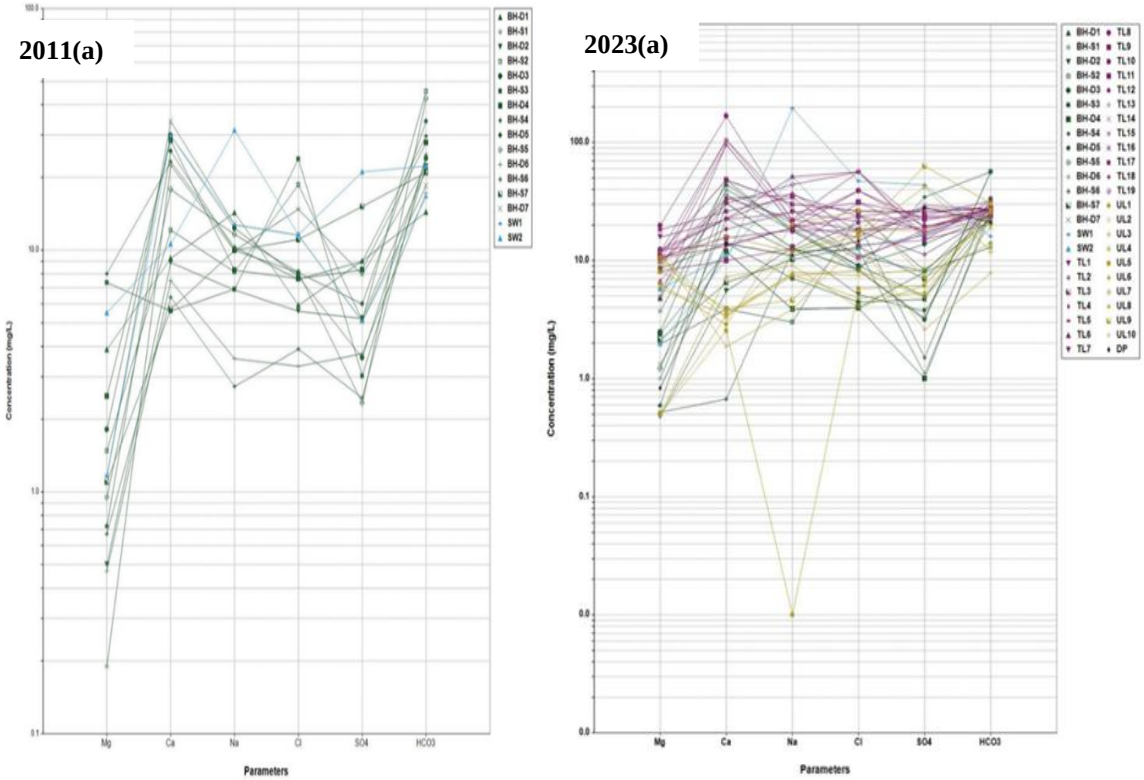

Fig. 2. Schoeller Diagram for Major Ions in 2011(a) and 2023(b)

4.3 Hydrochemical Facies of TSF Water, Surface Water and Groundwater

Trilinear Piper diagrams (Fig. 3) were used to evaluate the hydrochemical facies and geochemical evolution of surface water, groundwater, and tailings storage facility (TSF) waters between 2011(Fig. 3(a)) and 2023(Fig. 3()). In 2011, the overall hydrochemistry was dominated by Ca–HCO_3 facies (56.2%), with Ca–Cl (18.8%) and Na–SO_4 (13%) as secondary types, while smaller proportions of Na–HCO_3 (6%) and Mg–Cl (6%) were also recorded. By 2023, the system shifted markedly towards sulphate-rich waters, with Mg–SO_4 (23%), Ca–SO_4 (13%), and Na–SO_4 (12%) together accounting for almost half of the total composition, although Ca–HCO_3 (26%) remained significant (Gibbs, 1970).

At the individual water sources, surface water displayed the most dynamic changes. In 2011, surface water was characterised by Na–SO_4^{2-} and Ca–Cl facies (50% each). By 2023, the chemistry had evolved into Na–SO_4^{2-} (50%) and Na–HCO_3 (50%) types, indicating increasing anthropogenic influence. The persistence of sulphate facies points to contributions from sulphide oxidation and possible TSF seepage (Freeze and Cherry, 1979).

Groundwater exhibited more gradual changes. In 2011, Ca–HCO_3 (50%) was dominant, with subordinate Na–HCO_3 (14%) and Ca–Cl (14%). By 2023, Ca–HCO_3 remained the prevailing type (50%), accompanied by Ca–Cl (16.7%) and Na–HCO_3. The dominance of Ca–HCO_3 facies throughout the study period reflects natural buffering by carbonate and silicate weathering (Hem, 1989). Nonetheless, the appearance of Ca–Cl waters in 2023 suggests localised mixing with surface water or seepage from the TSF, demonstrating that the aquifer retains a degree of protection but is not entirely unaffected (Kovalevsky et al., 2004).

TSF waters showed the most pronounced transformation. In 2011, data were not available for TSF water characterisation. By 2023, however, the chemistry was dominated by sulphate facies, with Mg–SO_4 (50%), Ca–SO_4 (25%), and Na–SO_4 (20%), consistent with sulphide oxidation within the tailings and the release of sulphate-rich leachates (Lottermoser, 2010; Younger et al., 2002).

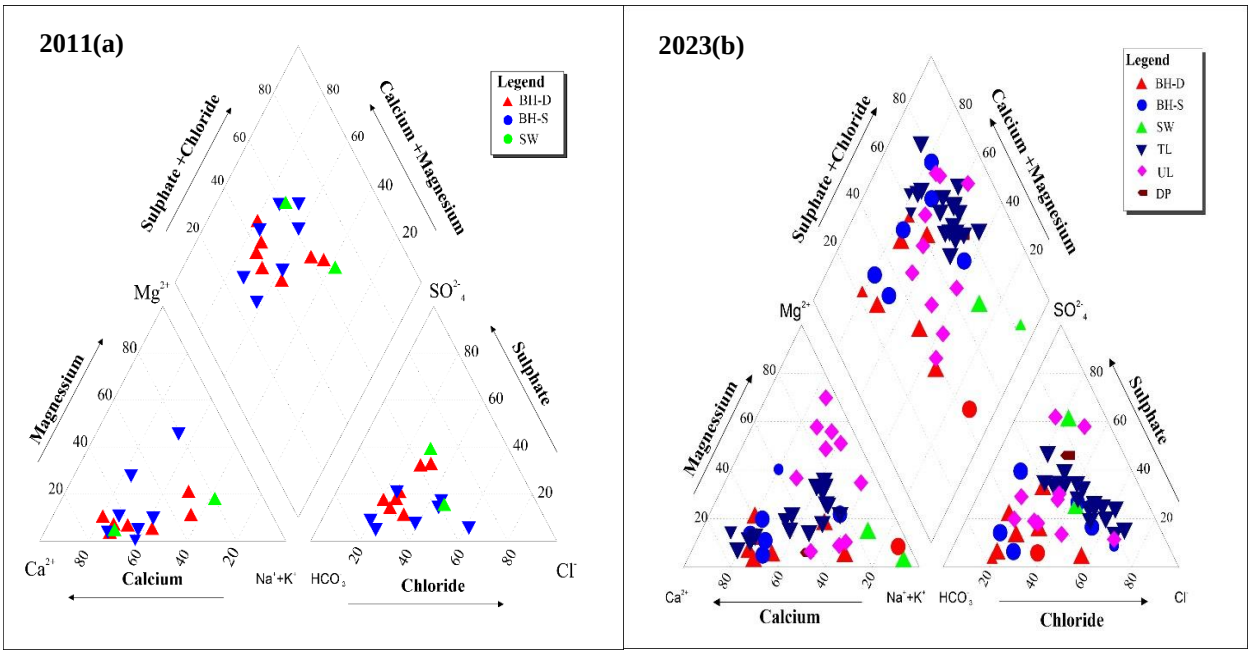

Fig. 3. Piper diagram illustrating the groundwater evolution and hydrochemical facies in 2011(a) and 2023(b)

4.4 Factors controlling groundwater chemistry

Gibbs diagrams (Figs. 4 and 5), illustrating the ratios of $Na^+/(Na^+ + Ca^{2+})$ and $Cl^-/(Cl^- + HCO_3^-)$ as functions of total dissolved solids (TDS), are widely employed to identify the dominant mechanisms controlling water chemistry namely, precipitation dominance, rock weathering dominance, and evaporation dominance.

In this study, chemical data from all sampling points between 2011 and 2023 were plotted on Gibbs diagrams. The clustering patterns of the sample points indicate that the chemical composition of groundwater is primarily governed by the weathering of rock-forming minerals. This finding suggests that mineral dissolution resulting from rock–water interactions is the principal process influencing the region's groundwater chemistry.

A few groundwater samples exhibited precipitation-dominated characteristics, including BH7S in 2011. The Gibbs plots further reveal a positive relationship between elevated TDS values and higher $Na^+/(Na^+ + Ca^{2+})$ ratios, implying that cation exchange processes involving sodium (Na^+) and calcium (Ca^{2+}) significantly contribute to the observed variations in groundwater chemistry.

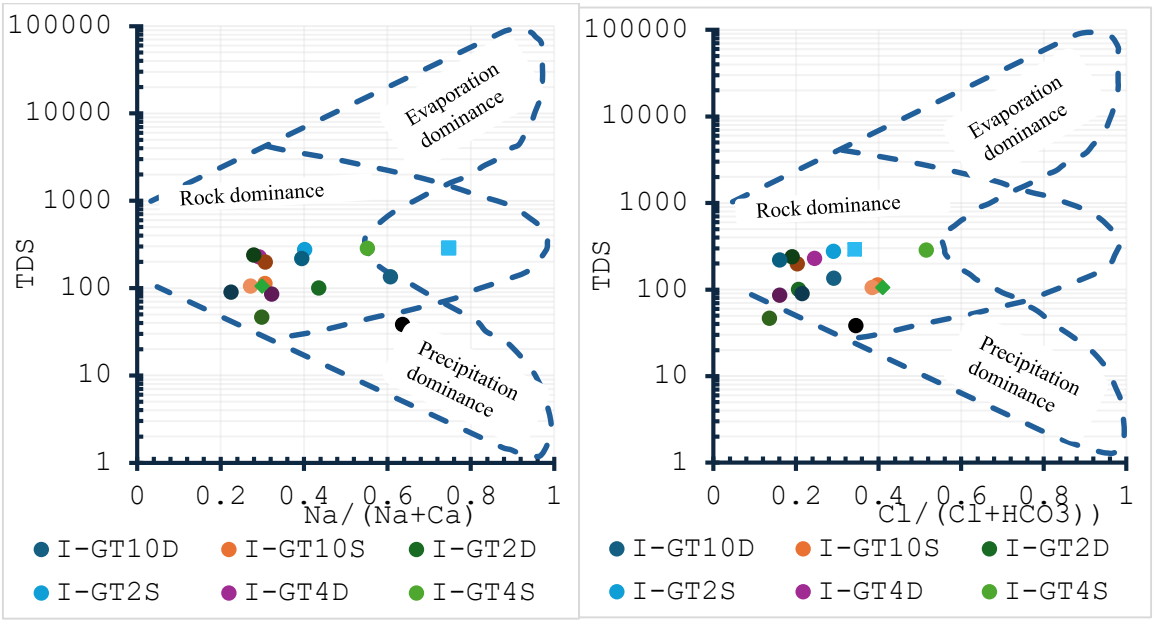

Fig. 4. Gibbs Plot Showing Factors Controlling Water Chemistry for 2011

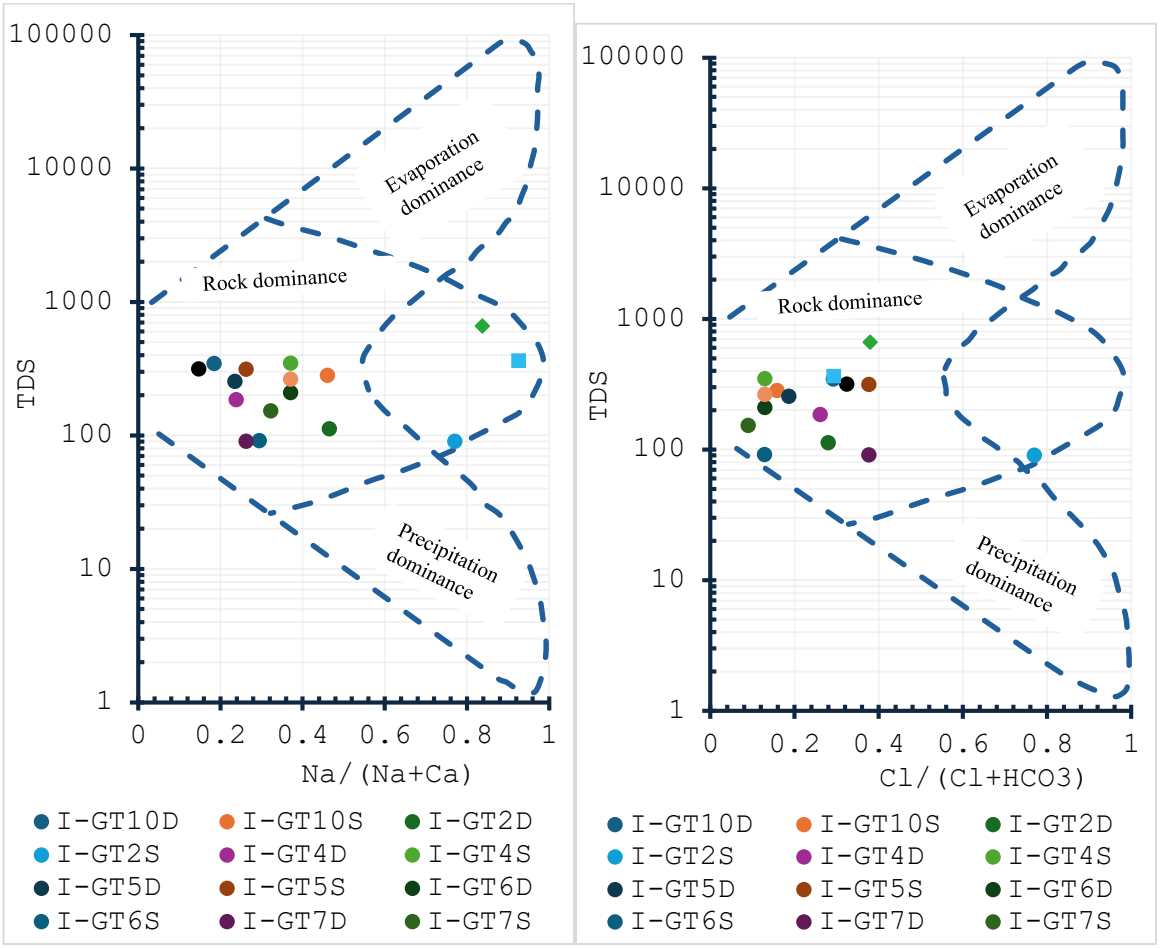

Fig. 5. Gibbs Plot Showing Factors Controlling Water Chemistry for 2023

The bivariate plots (Fig. 6) for 2011 illustrate the relationships among key ionic ratios used to infer hydrogeochemical processes governing groundwater evolution. The plot of Ca^{2+}/Mg^{2+} versus HCO_3^-/SO_4^{2-} exhibits a weak positive correlation (r = 0.216), with most samples plotting above the 1:1 line. This pattern suggests the occurrence of reverse ion exchange processes. In the Na^+ versus Cl^- plot, most samples cluster near the equiline, indicating halite dissolution as a major source of sodium and chloride ions.

In the Na^+ versus HCO_3^- plot, samples plotted close to the equiline imply carbonate mineral dissolution, supported by a modest positive correlation (r = 0.309). Similarly, the Na^+ versus $Na^+/(Na^+ + K^+)$ relationship reveals a positive correlation (r = 0.209), with samples near the equiline indicating silicate weathering, whereas those plotted above the 1:1 line suggests reverse ion exchange. Samples diverging above or below the equiline likely reflect reverse or forward ion exchange reactions, respectively.

The bivariate plot of Mg^{2+}/Ca^{2+} versus Ca^{2+}/Na^+ demonstrates a strong positive correlation (r = 0.996), with most samples distributed above the 1:1 line between silicate weathering and carbonate dissolution fields, indicating the concurrent influence of both processes. Similarly, the plot of HCO_3^-/Na^+ versus Ca^{2+}/Na^+ shows most samples clustered within the silicate and carbonate dissolution domains, supported by a very strong positive correlation (r = 0.999) between the x- and y-axis parameters. These relationships collectively suggest that groundwater chemistry in 2011 was primarily controlled by silicate and carbonate mineral weathering, with secondary contributions from ion exchange processes.

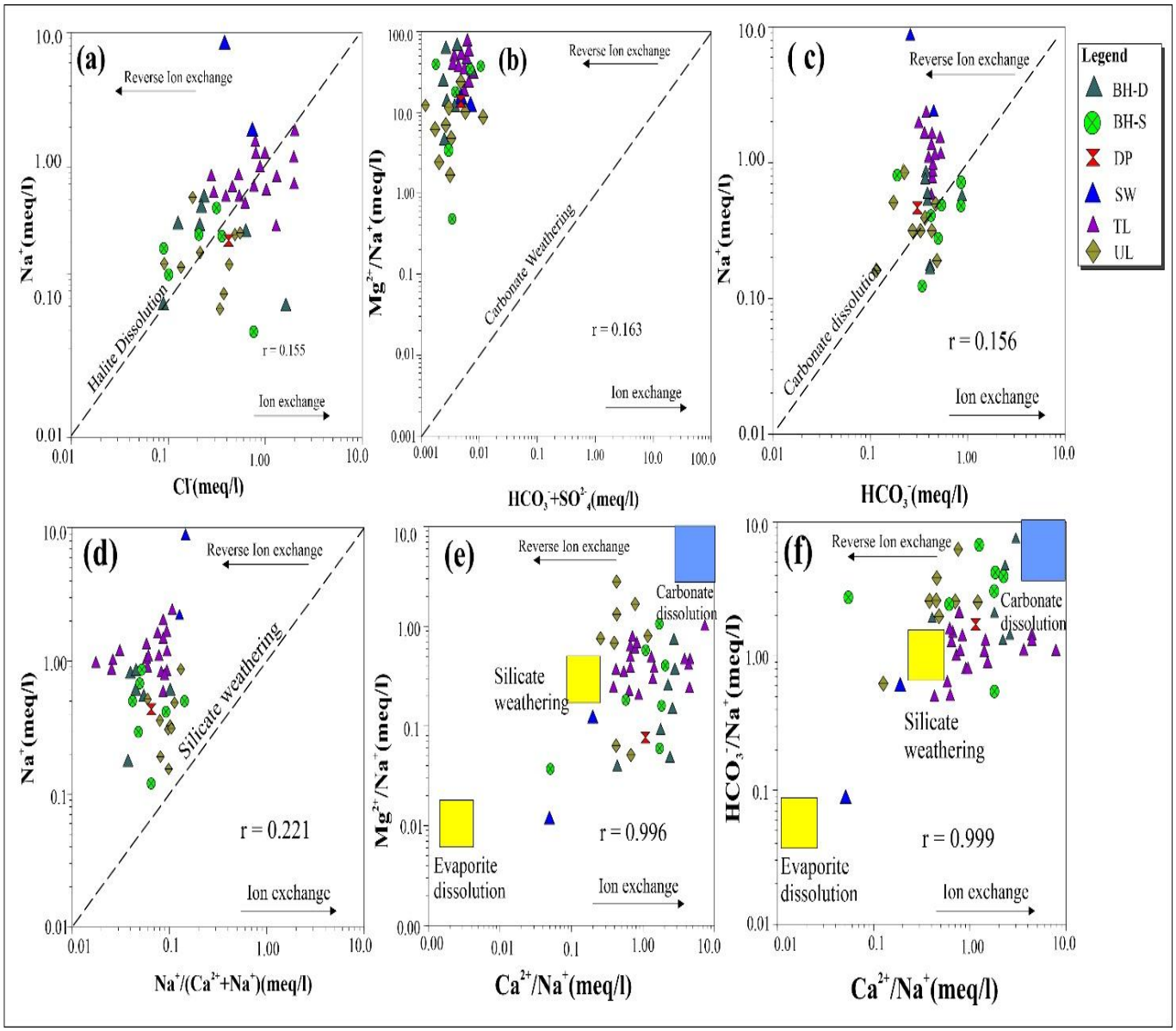

Fig. 6. Major element relationship depicting primary processes influencing groundwater chemistry

4.5 Sources of groundwater constituents

Factor analysis was conducted to determine the principal physicochemical parameters and variables influencing water quality within the study area. A total of twenty-one (21) physical, chemical, and metal variables were assessed for TSF water, surface water, and groundwater across the study years, from which four dominant factors were extracted for each period.

In 2011 (Fig. 7), the first component, with an eigenvalue of 0.975, explained 38.8% of the total variance, while the second (0.824), third (0.877), and fourth (0.903) components accounted for 17.4%, 11.3%, and 9.7% of the variance, respectively. In 2016, the first component (0.934) explained 42.5% of the variance, followed by the second (0.991) at 17.2%, the third (0.976) at 10.7%, and the fourth (0.733) at 6.4%. For 2017, the first component (0.940) contributed 43.4% of the total variance, with the second and third components (0.979 each) explaining 19.7% apiece, and the fourth (0.830) accounting for 6.2%. By 2023 (Fig. 8), the first component (0.952) explained 43% of the total variance, followed by the second (0.973) at 13.1%, the third (0.854) at 19.7%, and the fourth (0.797) at 7%.

These factors loading reflect the clustering of parameters associated with various hydrochemical processes contributing to the progressive mineralization of water. The identified components underscore the complex interplay between natural (geogenic) and human-induced (anthropogenic) factors influencing the hydrochemistry of the TSF, surface water, and groundwater systems. The results of the factor analysis thus provide critical insights into the dominant geochemical processes controlling water quality variations across temporal scales.

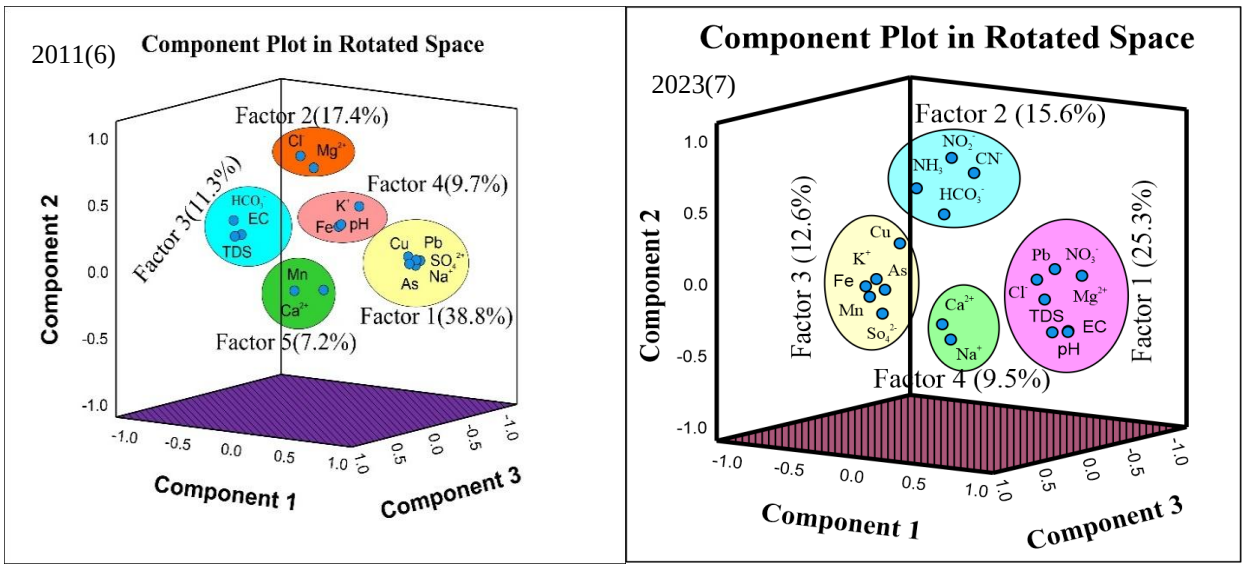

Fig. 7 and 8 Rotation plot of factor analysis using varimax rotation iteration

4.6 Hydrochemical Facies Correlation and Impacts Assessment

The entire perimeter of the GTSF was subdivided into four sections to enable correlation of hydrochemical facies across the various sampling media, including shallow and deep boreholes, underliner and topliner sumps, surface water bodies, and the decant pool (Figures 9–12). Distinct water types were represented using a standardised colour-coding scheme, with $CaSO_4$-dominated facies (decant water) indicated in red. Under optimal TSF construction, tailings water is expected to remain fully contained, minimising interaction with groundwater and surface water. However, the occurrence of similar water types across sampling points indicates potential hydraulic connectivity or geochemical interaction.

Along the northern section of the GTSF (Figure 9, AA′), potential geochemical interaction was inferred between topliner sump TL15 and underliner sump UL9, both exhibiting $CaSO_4$ facies (red code). This suggests a possible shared contamination pathway.

In the eastern section (Figure 9, AA′), groundwater sample UL9 and TSF water (TL16) exhibited the same $CaSO_4$ facies, while UL10 and TL16 shared a $NaHCO_3$ facies (yellow code), indicating interaction. In the southern section (Figure 9, CC′), a possible geochemical link was identified between groundwater (UL2) and TSF water (TL16), both showing MgCl facies (black code).

In the western section (Figure 11, DD′), surface water SW2 and TSF water (TL13) exhibited the same facies, suggesting interaction. Similarly, in the eastern section (Figure 10, BB′), topliner samples TL3, TL6, TL8, TL5 and groundwater borehole BHS1 (Figure 11, CC′) all exhibited CaCl facies (dark blue code), indicating potential mixing between surface water, groundwater, and TSF water.

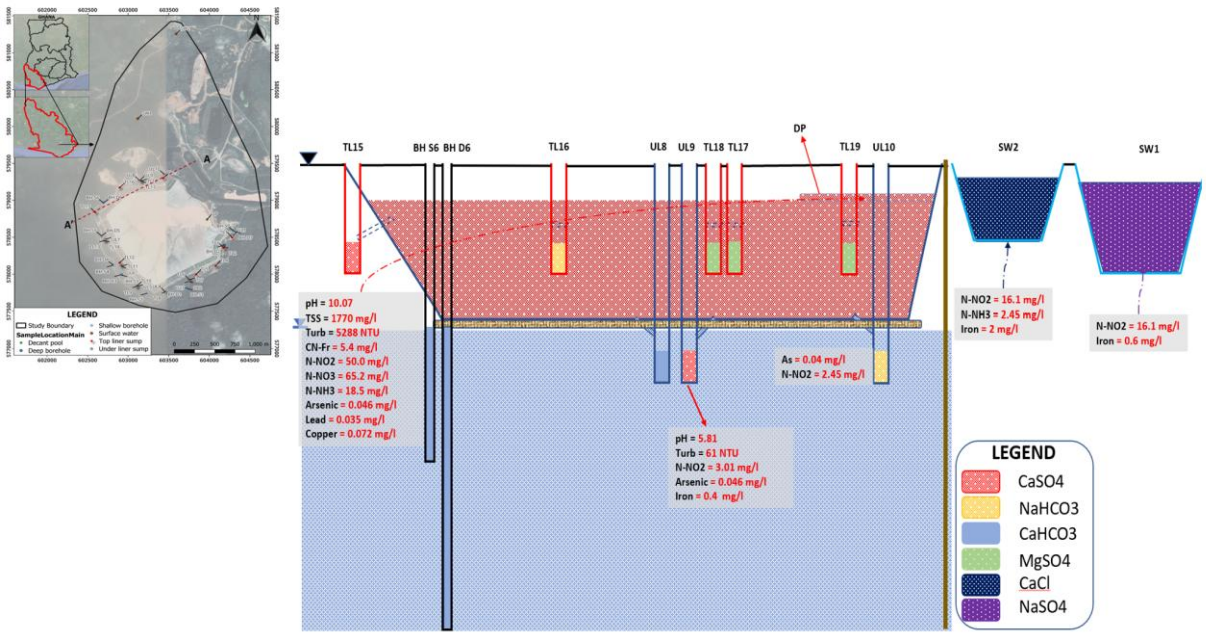

Fig. 9. AA' Hydrochemical Sectional View of the GTSF

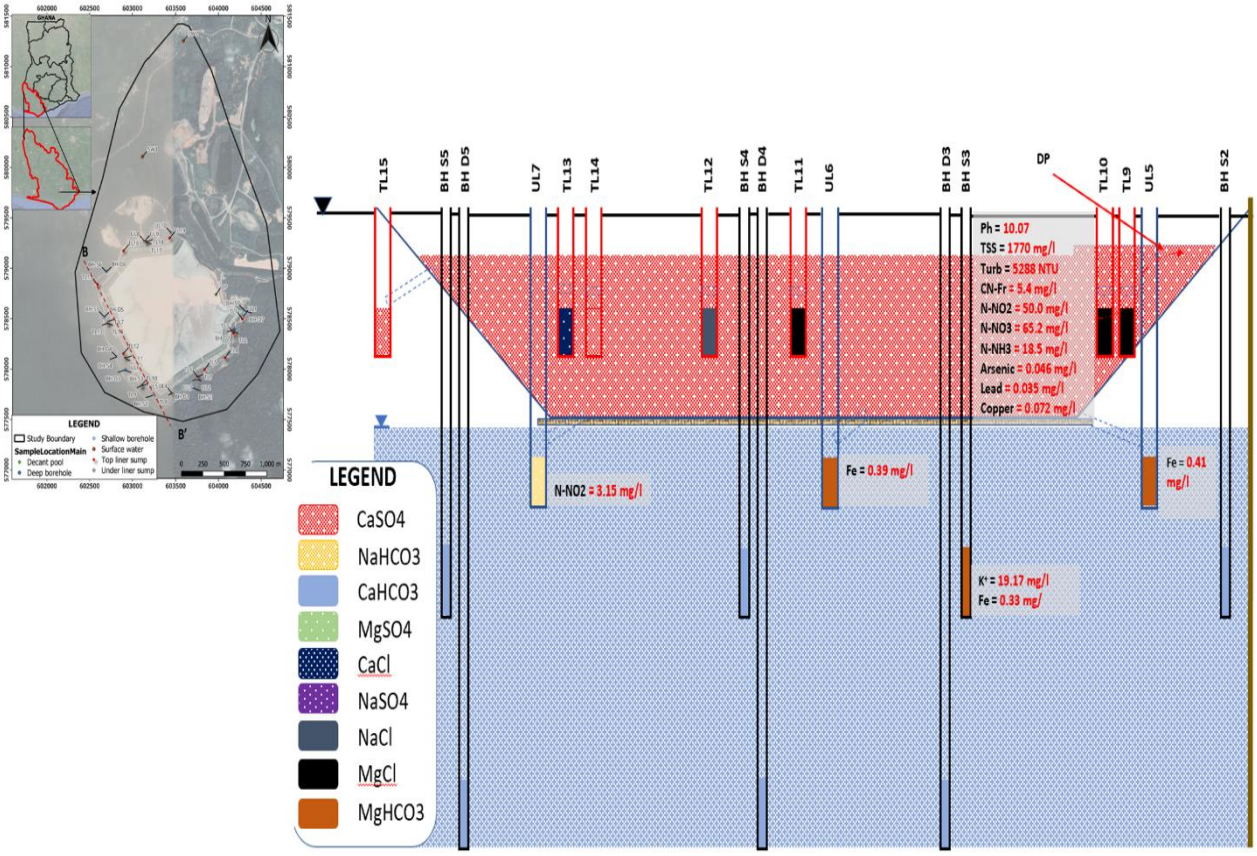

Fig. 10. BB' Hydrochemical Sectional View of the GTSF

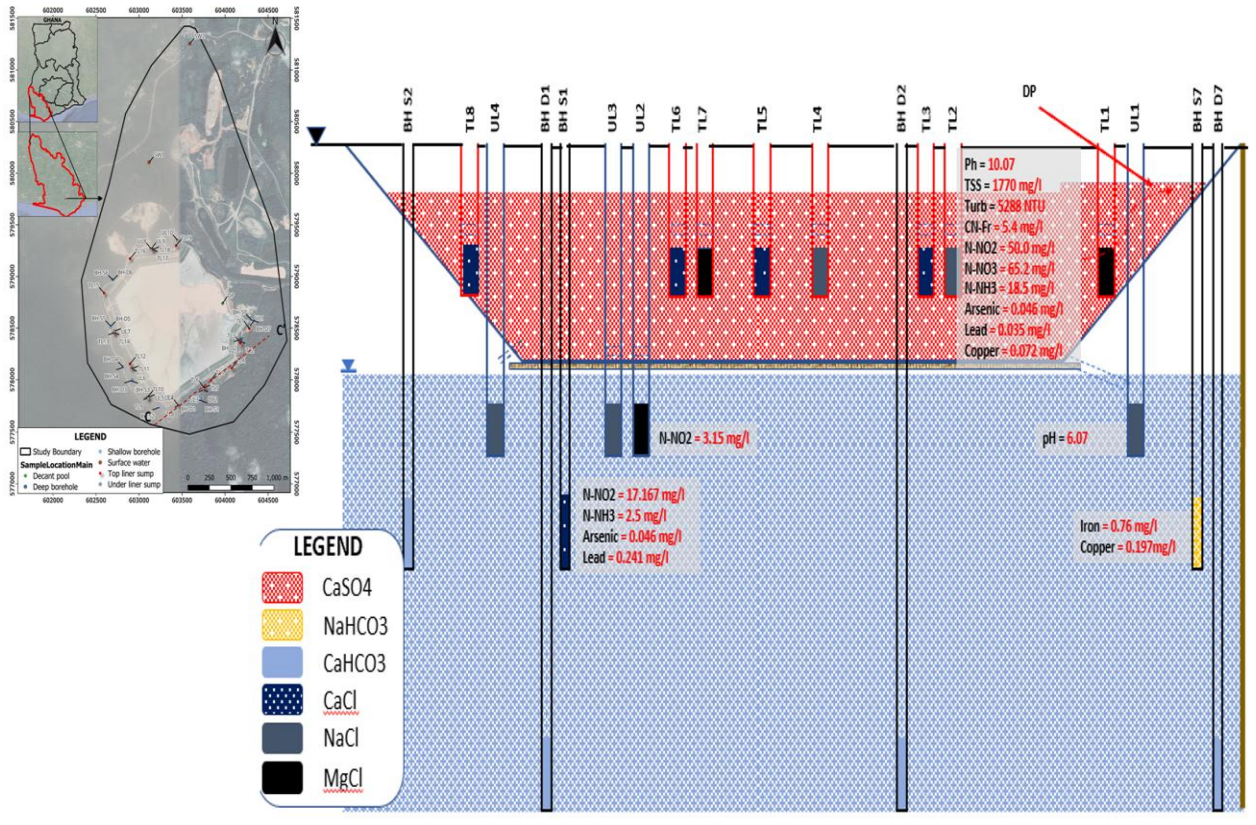

Fig. 11. CC' Hydrochemical Sectional View of the GTSF

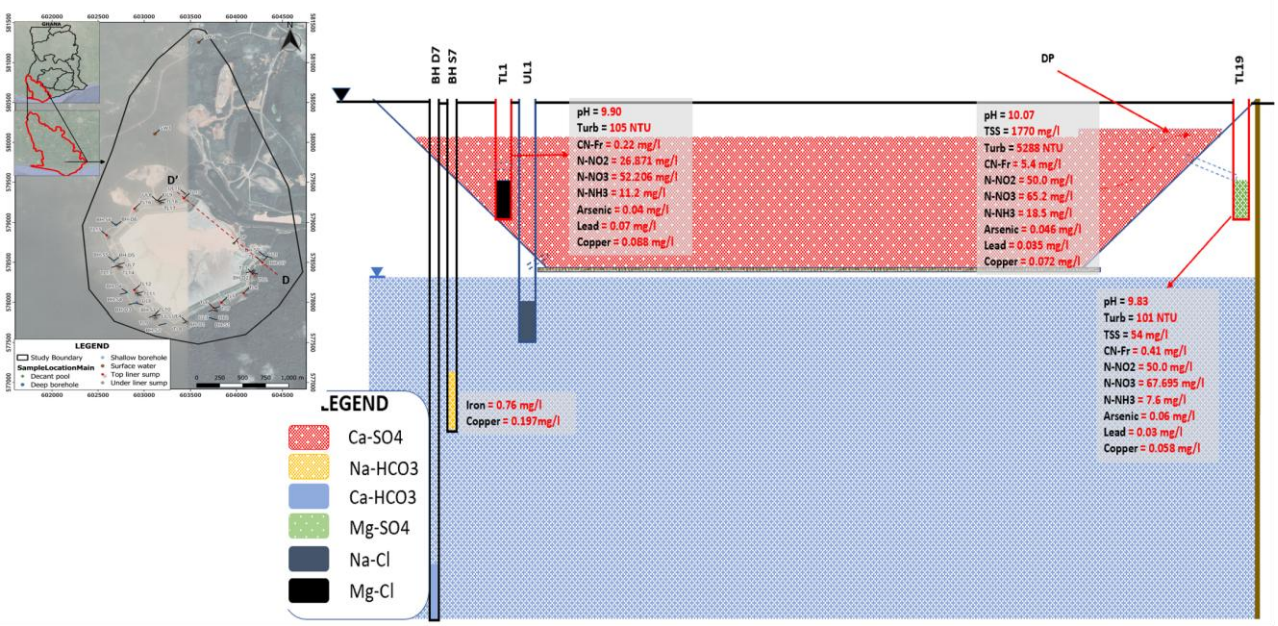

Fig. 12. DD' Hydrochemical Sectional View of the GTSF

4.7 Approaches for Decommissioning of TSF

The Greenfields Tailings Storage Facility (GTSF), covering a total area of approximately 245 ha, was constructed as an upstream development with tailings spigotting as the primary depositional method. The geometry and depositional history of the facility present unique challenges for decommissioning, particularly regarding water management, long-term stability, and protection of groundwater and surface water resources. A phased and prioritised approach is therefore essential, combining engineering solutions, water treatment, and ecological integration to ensure safe closure and post-mining land use (Anon, 2012; Lottermoser, 2010). The following innovative steps are proposed as part of the decommissioning strategy, arranged in order of importance and technical sequence:

i. Dewatering and Water Management

Hydrochemical assessment indicates that several water quality parameters (pH, TSS, potassium, cyanide, ammonia, arsenic, lead, iron, copper) exceed the acceptable limits set by the Environmental Protection Agency (EPA), Ghana Standards Authority (GSA), and World Health Organization (WHO). Continuous pumping from the decant pool, topliner drains, and shallow and deep groundwater monitoring wells into a 39 ha central sump will be undertaken. Dewatering will continue until water quality parameters consistently meet regulatory standards. This step reduces hydraulic head, enhances structural stability, and prevents further seepage (Anon., 2017).

ii. Advanced Water Treatment

Water collected in the sump will undergo multi-stage treatment. The process involves coagulation and flocculation to remove suspended solids, pH adjustment with sulphuricacid (H_2SO_4), cyanide destruction using sodium metabisulphite with ferric chloride as a catalyst, followed by reverse osmosis to remove dissolved metals and salts. This treatment ensures compliance with EPA, GSA, and WHO discharge standards and provides protection for downstream users (Younger, Banwart and Hedin, 2002).

iii. Recycling, Reuse, and Controlled Discharge

Treated water that meets acceptable standards will be preferentially reused in the gold processing plant, reducing the demand for fresh water. Surplus water will either be discharged under EPA permits or stored for auxiliary uses such as dust suppression and site irrigation. This promotes a circular water economy and minimises environmental discharge risks (Ritcey, 2005).

iv. Encapsulation and Physical Stabilisation

To prevent oxygen ingress and water infiltration, which could trigger acid mine drainage and contaminant leaching, the GTSF surface will be encapsulated with 500 mm layer of topsoil across the facility, providing a growth medium for vegetation. This cover system stabilises the tailings surface, reduces erosion risk. The use of topsoil capitalises on available resources while promoting ecosystem restoration (Lottermoser, 2010).

v. Establishment of Buffer Zones

Vegetated buffer strips will be created around sensitive surface water bodies adjacent to the TSF. These zones act as a final filter for residual surface runoff, protect aquatic ecosystems, and provide landscape integration. They also enhance biodiversity and reduce the visual footprint of the closed facility (Anon., 2017).

vi. Monitoring Routine monitoring will involve scheduled sampling of groundwater from boreholes and adjacent surface water bodies to evaluate water quality trends. A structured maintenance programme will also be implemented to address issues such as erosion, vegetation dieback, and potential seepage concerns (Mayer and MacQuarrie, 2010; Steefel et al., 2015).

5. CONCLUSION

This study comprehensively examined the hydrochemical evolution and interrelationships among groundwater, surface water, and tailings storage facility (TSF) water within the Greenfields area from 2011 to 2023. The research integrated geochemical, statistical, and spatial analyses to assess water quality, determine dominant controlling processes, and evaluate the degree of interaction among the three water systems. The findings revealed a complex interplay of geogenic and anthropogenic influences driven by rock–water interactions, mining activities, and tailings seepage dynamics.

Analysis of water quality data showed that several physical parameters (pH, TSS, turbidity), chemical constituents (potassium, cyanide, ammonia), and metallic elements (arsenic, lead, iron, copper, manganese) exceeded the permissible limits set by the Environmental Protection Agency (EPA), Ghana Standards Authority (GSA), and World Health Organization (WHO) for both surface and groundwater. These exceedances highlight the cumulative impacts of tailings seepage, mineral oxidation, and anthropogenic inputs on water quality within and around the TSF.

Interpretation of Gibbs diagrams indicated that rock–water interaction and mineral weathering are the principal processes governing the overall water chemistry in the study area. However, precipitation dominance was observed in specific shallow and deep boreholes particularly BH2, BH5, and BH7suggesting localized recharge zones and seasonal dilution effects that contribute to hydrochemical variability across the site.

Piper diagram analysis revealed that the Ca–HCO_3 water type predominates within the groundwater system, reflecting carbonate weathering as the major geochemical process. Secondary facies such as Ca–Cl and Na–HCO_3 indicate progressive ion exchange and minor saline intrusion, consistent with limited but measurable influence from the TSF in certain locations.

Principal Component Analysis (PCA) identified pH, EC, TDS, NO_3^-, NO_2^-, NH_3, Fe, Mn, SO_4^{2-}, and CN^- as the dominant parameters contributing to hydrochemical variability. Strong correlations among these variables demonstrate the combined effects of natural geochemical evolution and anthropogenic contamination, particularly from cyanide use, ammonia volatilization, and dissolved solids derived from tailings oxidation and seepage.

Hydrochemical facies correlation and impact assessment confirmed zones of hydraulic connectivity and geochemical mixing between the TSF, groundwater, and surface water systems. The recurrence of similar facies such as Ca–SO_4, Mg–Cl, and Ca–Cl—across topliners, underliners, and adjacent boreholes provides strong evidence of seepage migration pathways and chemical exchange between the TSF and surrounding aquifers.

The decommissioning of a TSF can be effectively achieved through six integrated approaches: systematic dewatering of decant water, treatment of both decant and impacted groundwater, recycling, reuse, and controlled discharge of treated water, encapsulation and stabilization of the TSF, establishment of protective buffer zones for surface water, and implementation of long-term care, maintenance, and monitoring programs.

REFERENCES

1. Aitchison, J. and Greenacre, M. (2002) 'Biplots of compositional data', Journal of the Royal Statistical Society: Series C (Applied Statistics), 51(4), pp. 375–392.
2. Al-Hassan, S.A. (2007) 'Comparative study of rainfall in Tarkwa mining district of Ghana', Ghana Mining Journal, 9, pp. 25–32.
3. Franks, D.M., Boger, D.V., Cote, C.M. and Mulligan, D.R. (2011) 'Sustainable development principles for the disposal of mining and mineral processing wastes', Resources Policy, 36, pp. 114–122.
4. Freeze, R.A. and Cherry, J.A. (1979) Groundwater. Upper Saddle River, NJ: Prentice-Hall Inc., p. 604.
5. Gibbs, R.J. (1970) 'Mechanisms controlling world water chemistry', Science, 170(3962), pp. 1088–1090.
6. Hem, J.D. (1989) Study and interpretation of the chemical characteristics of natural water. U.S. Geological Survey Water-Supply Paper 2254.
7. Kovalevsky, V.S., Kruseman, G.P. and Rushton, K.R. (eds.) (2004) Groundwater studies: an international guide for hydrogeological investigations. Paris: United Nations Educational, Scientific and Cultural Organization (UNESCO).
8. Li, P., Wu, J. and Qian, H. (2015) 'Hydrochemical appraisal of groundwater quality for drinking and irrigation purposes and the major influencing factors: a case study in and around Hua County, China', Arabian Journal of Geosciences, 9(1), p. 15.
9. Lottermoser, B.G. (2010) Mine wastes: characterization, treatment and environmental impacts. 3rd edn. Berlin: Springer-Verlag.
10. Sunkari, E.D., Okyere, M.B., Adams, S.J., Zango, M.S., Bhattacharya, P. and Ali, S. (2023) 'Geochemical controls on fluoride enrichment in groundwater of a geologically heterogeneous part of Ghana: implications for human health risk assessment', in Ali, S. and Negm, A. (eds.) Groundwater quality and geochemistry in arid and semi-arid regions. The Handbook of Environmental Chemistry, vol. 126. Cham: Springer, pp. 297–326.
11. Sunkari, E.D., Zango, M.S., Abu, M., Adomako, D. and Osae, S. (2020) 'Hydrogeochemical evolution

and groundwater quality assessment in a mining basin, southwestern Ghana', Groundwater for Sustainable Development, 10, p. 100325.

12. World Health Organization (WHO) (2022) Guidelines for drinking-water quality. 4th edn incorporating the 1st and 2nd addenda. Geneva: World Health Organization.
13. Younger, P.L., Banwart, S.A. and Hedin, R.S. (2002) Mine water: hydrology, pollution, remediation. Dordrecht: Kluwer Academic Publishers.
14. Zango, M.S., Sunkari, E.D., Abu, M. and Lermi, A. (2019) 'Hydrogeochemical controls and human health risk assessment of groundwater fluoride and boron in the semi-arid North East region of Ghana', Journal of Geochemical Exploration, 207, p. 106363.